

Introduction

A *granular material* is a collection of solid particles or grains, such that most of the particles are in contact with at least some of their neighboring particles. The terms “granular materials,” “bulk solids,” “particulate solids,” and “powders” are often used interchangeably in the literature. Common examples of granular materials are sand, gravel, food grains, seeds, sugar, coal, and cement. Figure 1.1 shows the typical size ranges for some of these materials.

Granular materials are commonly encountered in nature and in various industries. For example, with reference to the chemical industry, Ennis et al. (1994) note that about 40% of the value added is linked to particle technology. Similarly, Bates (2006) notes that more than 50% of all products sold are either granular in form or involve granular materials in their production. In spite of the importance of granular materials, their mechanics is not well understood at present. Nevertheless, some progress has been made during the past few decades. The goal of this book is to describe some of the experimental observations and models related to the mechanical behavior of *flowing* granular materials. As studies in this area are increasing rapidly, our account is necessarily incomplete. However, it is hoped that the book will provide a useful starting point for the beginning student or researcher.

A material is called a *dry* granular material if the fluid in the interstices or voids between the grains is a gas, which is usually air. On the other hand, if the voids are completely filled with a liquid such as water, the material is called a *saturated* granular material. If there is a liquid in some of the voids, and the rest of the voids are filled with a gas, the material is said to be *partially saturated*. For example, the upper region of a soil in its natural environment is usually partially saturated, whereas the lower region is saturated. In the recent literature, both saturated and partially saturated materials are called *wet* granular materials.

If the particles lose contact with each other, and each particle is surrounded by a fluid, the granular material becomes a *fluid–particle suspension*. At present, a unified theory for the mechanical behavior of granular materials and suspensions is lacking. In this book, attention will be confined to the former, barring a brief discussion of some aspects of the latter in this chapter. The reader is referred to Gidaspow (1994), Fan and Zhu (1998), and Jackson (2000) for a detailed discussion of suspensions.

When granular materials are at rest, or in motion, they exhibit many features which cannot be anticipated on the basis of our experience with fluids such as air and water, and solids such as steel and wood. Like solids, they can sustain shear stresses at rest, as in the case of a heap or “sandpile.” In a heap formed by pouring a free-flowing granular material from a funnel onto a flat surface, the inclination of the free surface of the heap to the horizontal cannot be arbitrary but is limited by a maximum value called the *angle of repose*. Like liquids, they flow from vessels under the action of gravity, but the mass flow rate is approximately independent of the height of material above the discharge orifice. This

Introduction

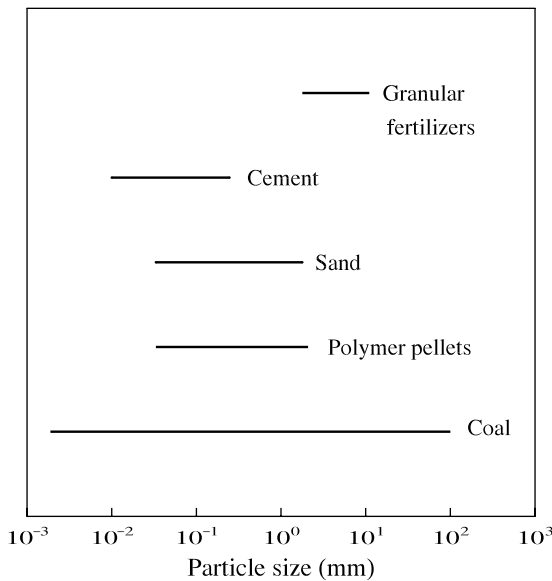


Figure 1.1. Size ranges of various granular materials. (Data taken from Fedá, 1982, p. 22, and Brown and Richards, 1970, pp. 4–8.)

feature accounts for the use of hourglasses containing sand as clocks a few centuries ago. Unlike water, granular materials are compressible in the sense that the space between the particles often changes during flow. For example, if the particles are tightly packed, they tend to move apart when they flow. Whereas water and alcohol can be readily mixed to obtain a liquid of uniform composition, attempts to mix particles of two sizes or of two materials often lead to segregation or separation of the constituents.

In some cases, particularly when dealing with coarse materials, the effect of the interstitial fluid can be ignored. In other cases, such as the flow of fine granular materials through a long vertical pipe connected to a storage vessel above it, fluid–particle interaction strongly affects the flow rate of particles.

Overall, granular materials share some features of common fluids and solids but also differ from them in many ways. Various aspects of the behavior of granular materials have been discussed in review articles written by Jackson (1983, 1986), Jaeger and Nagel (1992), Hutter and Rajagopal (1994), Jaeger et al. (1996), de Gennes (1998), Roberts (1998), Sundaresan (2001), Hill and Selvadurai (2005), and Campbell (2006).

The outline of this chapter is as follows. Some examples of granular statics and flow are presented below, followed by a discussion of interparticle and fluid–particle forces. Some of the available models will be described briefly. Here it may be noted that the focus of the book is on continuum models. Finally, balance laws for such models will be formulated.

Some of the material presented in this and subsequent chapters requires a knowledge of vectors and tensors. Readers who are not familiar with these concepts will find a brief discussion in Appendices A and B.

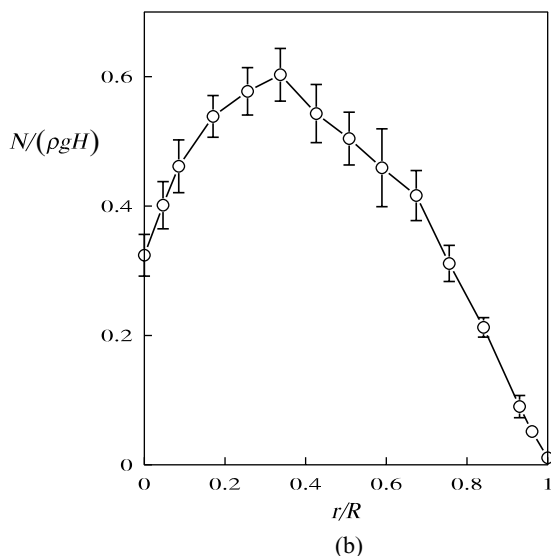
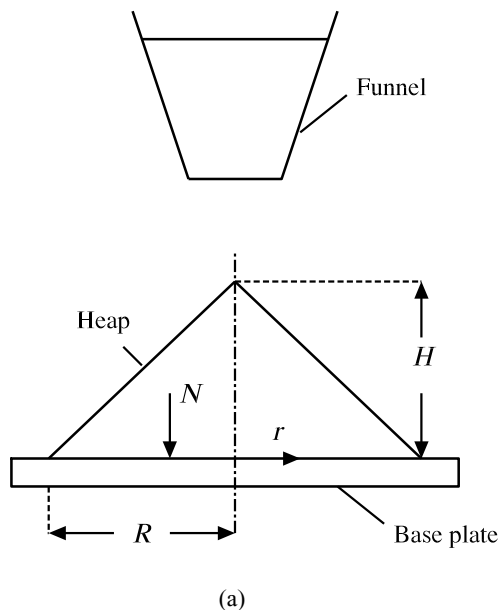
1.1. EXAMPLES OF GRANULAR STATICS AND FLOW

(a) *Heaps*

Consider a conical heap or pile of granular material resting on a horizontal surface. Several workers have measured the normal stress N exerted by the material on the base of the heap as a function of radial distance r measured from the center of the base. Here we discuss the results of Vanel et al. (1999) for heaps of sand. The heap was constructed by pouring sand from a funnel onto a base plate (Fig. 1.2a), with the funnel being moved upward so that its

Introduction

Figure 1.2. (a) A heap formed by pouring material from a funnel onto a circular metal plate. The funnel is raised so that its tip is always slightly above the apex of the heap. (b) Profile of the normal stress N exerted by the heap. The symbols represent the data of Vanel et al. (1999) for sand, with the vertical lines representing the standard deviation of several (typically 10–12) independent experiments. The piecewise linear curve is drawn to guide the eye. Here ρ is the density and g is the acceleration due to gravity. The lengths H , R , and r are measured as shown in (a). (Figure 1.2b has been reproduced from Vanel et al., 1999, with permission from Prof. R. P. Behringer and the American Physical Society. Copyright (1999) by the American Physical Society.)



tip was always slightly above the apex of the heap. The stress profile shows a minimum at the center of the base (Fig. 1.2b), contrary to the intuitive expectation that the normal stress should be a maximum at this location. This is called the *stress dip*, and several models have been proposed to explain such profiles (see, e.g., Cates et al., 1998; Didwania et al., 2000). It should be noted that the stress dip is not a universal feature. For example, when the heap was constructed by pouring material through a sieve that was slowly raised (Fig. 1.3a), the stress dip was not observed (Fig. 1.3b). Similarly, in the experiments of Brockbank et al. (1997), the dip occurred for small glass beads (mean diameter = 0.18 mm, standard deviation = 0.02 mm), but not for large glass beads (mean diameter = 0.56 mm, standard deviation = 0.05 mm).

Given a granular material and a procedure for constructing the heap, it is not yet possible to predict whether a stress dip will occur. Similarly, a simple physical explanation for the dip is not available. An explanation due to Vanel et al. (1999) is given below.

Introduction

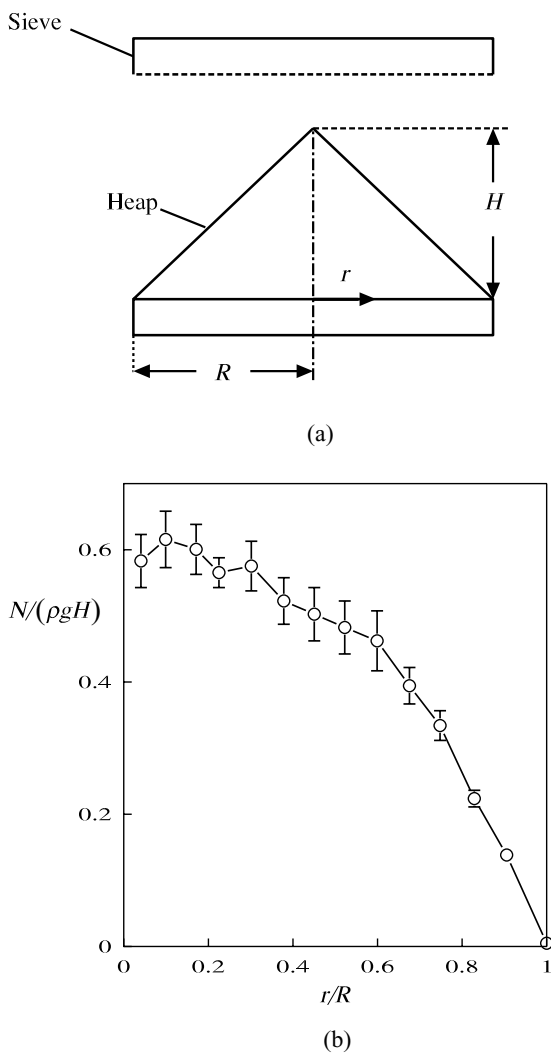


Figure 1.3. (a) A heap formed by pouring material from a sieve onto a circular metal plate. The sieve initially rests on the plate and is then raised gradually. (b) Profile of the normal stress N exerted by the heap. The symbols represent the data of Vanel et al. (1999) for sand, with the vertical lines representing the standard deviation of several (typically 10–12) independent experiments. The piecewise linear curve is drawn to guide the eye. Here ρ is the density and g is the acceleration due to gravity. The lengths H , R , and r are measured as shown in (a). (Figure 1.3b has been reproduced from Vanel et al., 1999, with permission from Prof. R. P. Behringer and the American Physical Society. Copyright (1999) by the American Physical Society.)

Experiments on static beds of granular materials show that the stresses are transmitted along preferred directions, which are called *force chains* or *stress chains* (see, e.g., Wakabayashi, 1957; Liu et al., 1995; Vanel et al., 1999). Figure 1.4 shows a two-dimensional pile of photoelastic disks. When viewed between crossed polarizers, the stress chains are visible as the bright stripes. As the chains are not vertical, Vanel et al. (1999) suggest that they may deflect a part of the weight away from the center of the base, leading to a stress dip. (A similar suggestion was made by Trollope (1968) and Edwards and Oakeshott (1989), who visualized the heap as being composed of arches, each of which supported its own weight.) Unfortunately, Vanel et al. (1999) do not show a picture of the chains for the case where a dip is not observed. Hence it is not known whether the pattern of chains differs significantly from that observed when there is a dip.

The occurrence of a stress dip has no analog in hydrostatics. Further, the measurements of Smid and Novosad (1981) show that unlike fluids, granular materials exert *nonzero* shear stresses on the base of a heap, even when they are at rest. Thus the statics of these materials is qualitatively different from that of fluids.

Introduction

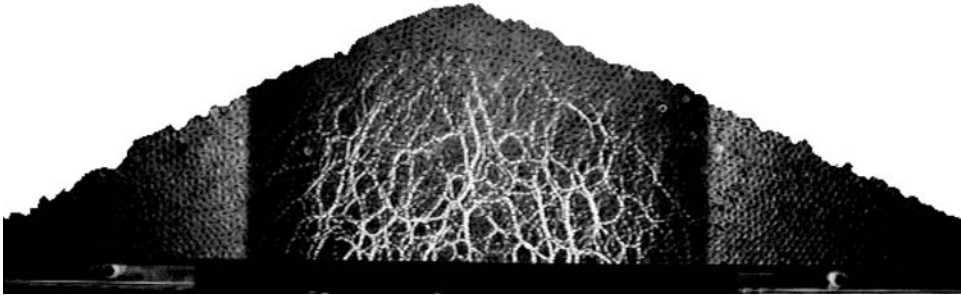


Figure 1.4. A heap formed by pouring photoelastic disks of two sizes from a funnel onto a plate. The apex of the heap is about 0.3 m above the base, and the diameters of the disks are 7.4 and 9 mm. The heap is viewed between crossed polarizers. (Reproduced from Vanel et al., 1999, with permission from Prof R. P. Behringer and the American Physical Society. Copyright (1999) by the American Physical Society.)

(b) Silos

Silos are vessels used for storing granular materials. Depending on their shapes, silos are also called bins, hoppers, or bunkers (Fig. 1.5). It has been found experimentally that the mass flow rate of coarse materials from silos is approximately independent of the head or height of material above the exit slot, provided the head is larger than a few multiples of the size of the exit slot. This is an unexpected result, if we note that the flow rate of water from vessels depends on the head. As discussed in Chapter 3, head independence arises from dry friction between the individual grains and between the grains and the wall of the silo.

Another feature of interest is the occurrence of several flow patterns when materials flow through bunkers. If the walls of the hopper section are sufficiently steep and the material is free flowing, *mass flow* occurs. Here all the material in the bunker is in motion (Fig. 1.6a). On the other hand, if the walls of the hopper section are shallow, *funnel flow* or *core flow* occurs. In the lower part of the bunker, there is a central core of rapidly moving material, surrounded by shoulders of material that is either stagnant or moving very slowly (Fig. 1.6b). The presence of stagnant and flowing zones makes it difficult to model such systems. It is likely that different sets of governing equations may be required for the two zones.

(c) Chutes

A chute is used to transport material by gravity flow from one point to another point at a lower level (Fig. 1.7a). Some features of chute flow can be illustrated by considering the experiments of Johnson et al. (1990). The chute is connected to a supply bunker containing glass beads by a chamber having valves at either end. By suitably adjusting the valves,

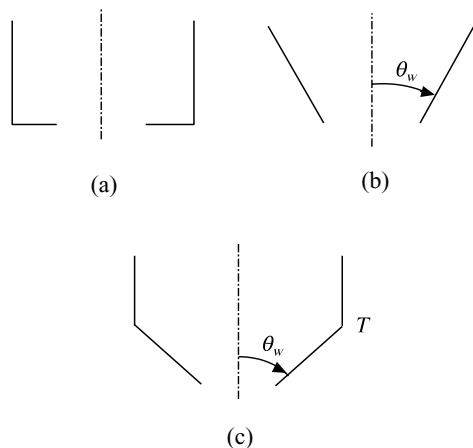


Figure 1.5. Shapes of silos: (a) bin, (b) hopper, and (c) bunker. In (c), T denotes the transition point.

Introduction

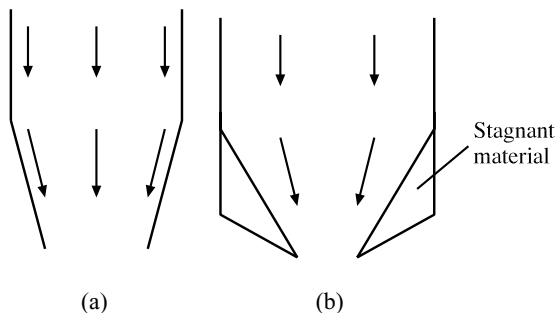


Figure 1.6. Flow patterns in bunkers: (a) mass flow and (b) funnel flow.

it is possible to regulate the mass flow rate of the beads and to permit two types of inlet conditions at the entry of the chute. These are termed (i) the dense entry condition and (ii) the loose entry condition. In case (i), the material enters the chute as a dense bed which moves slowly, whereas in case (ii), it enters as a low-density “cloud” of bouncing particles.

At locations that are not too close to the ends of the chute, it is found that quantities do not vary significantly in the flow direction, i.e., the flow is fully developed. This occurs for a range of inclinations of the chute. For fully developed flows, Fig. 1.7b shows the variation of the dimensionless mass flow rate per unit width of the chute \dot{m}^* with the dimensionless mass holdup m_T^* . The mass holdup is the mass of material contained between two planes normal to the flow direction (see the broken lines in Fig. 1.7a), divided by the corresponding area of the base. At low values of the flow rate, the holdup is found to be independent of the entry condition. As the flow rate increases from point 1, the density of the flowing layer increases. For flow rates higher than point 3, the holdup for the loose entry condition is much less than that for the dense entry condition, and the velocity profiles are also qualitatively different in the two cases. The horizontal arrow in the $\dot{m}^* - m_T^*$ plot in Fig. 1.7b indicates an abrupt transition from the loose entry branch to the dense entry branch as the flow rate is increased. This happens for certain values of the inclination θ . Considering the velocity profiles, it is seen that the slip velocity at the base of the chute can be quite large in some cases, in contrast to the behavior of liquids. Further, for dense entry flows (see the points 4' and 5' in Fig. 1.7b), only a part of the material above the base shears, and the rest appears to move like a plug.

Thus chute flows reveal many interesting features, such as multiple steady states, velocity slip at solid boundaries, and the occurrence of many types of density and velocity profiles.

(d) Vertical channels

Consider the flow of granular materials through a channel under the action of gravity (Fig. 1.8a). Far from the ends of the channel, the profile of the vertical velocity is found to be approximately independent of the vertical coordinate, and hence a fully developed state is attained, as in the case of fluids. The data of Nedderman and Laohakul (1980) for the flow of glass beads through a channel of rectangular cross section are shown in Fig. 1.8b. Near the center of the channel, the velocity profile is almost flat and the material moves like a plug. In the *shear layer* near the wall of the channel, the velocity varies significantly over a length scale that is of the order of 10 particle diameters. Flow fields containing both plug layers and shear layers occur in many devices such as bunkers, chutes, rotary drums, and shear cells.

(e) A standpipe connected to a hopper

A standpipe is a pipe used to convey particles from fluidized beds and hoppers. Figure 1.9a shows a hopper connected to a vertical standpipe and also a bare hopper, both of which are filled with sand. A photograph, taken soon after the sand was allowed to discharge

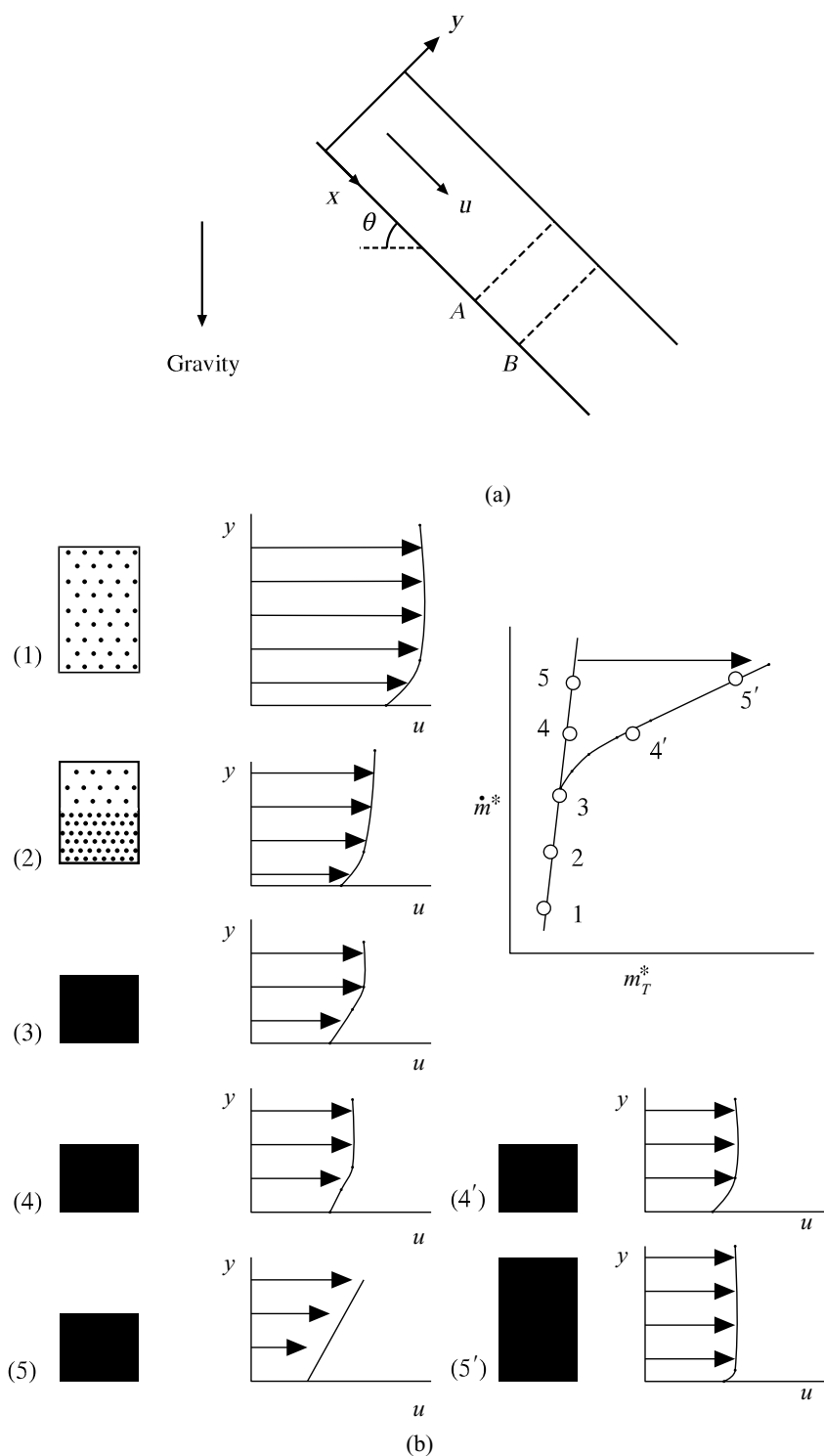


Figure 1.7. (a) Flow down a chute. (b) Variation of the dimensionless mass flow rate per unit width \dot{m}^* with the dimensionless mass holdup m_T^* for the flow of glass beads (Johnson et al., 1990). The flow rate is scaled by $\rho_p d_p \sqrt{g d_p}$, and the holdup by $\rho_p d_p$, where ρ_p is the particle density, d_p is the particle diameter, and g is the acceleration due to gravity. Points 4 and 5 correspond to the loose entry condition and 4' and 5' to the dense entry condition. For points 1–3, the holdup is independent of the entry condition. The profiles of the x component of velocity u are also shown. The shaded boxes indicate the distribution of the solids fraction in the y direction. The particle diameter is 1 ± 0.1 mm. (Figure 1.7b has been reprinted from Johnson et al., 1990, with permission of Cambridge University Press.)

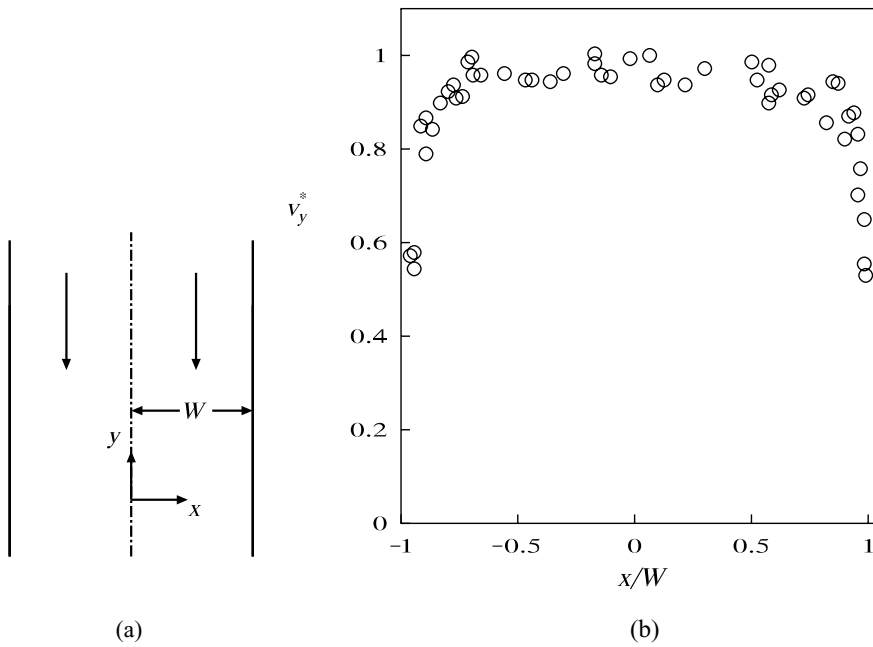


Figure 1.8. (a) Flow through a vertical channel. (b) Profile of the scaled vertical velocity $v_y^* \equiv v_y(x, y_1)/v_y(0, y_1)$ for glass beads, at some vertical position $y = y_1$ within the fully developed region. Data of Nedderman and Laohakul (1980) for a channel with glass faces and wooden side walls. Parameter values: particle diameter $d_p = 2$ mm, half-width of the channel $W = 60$ mm.

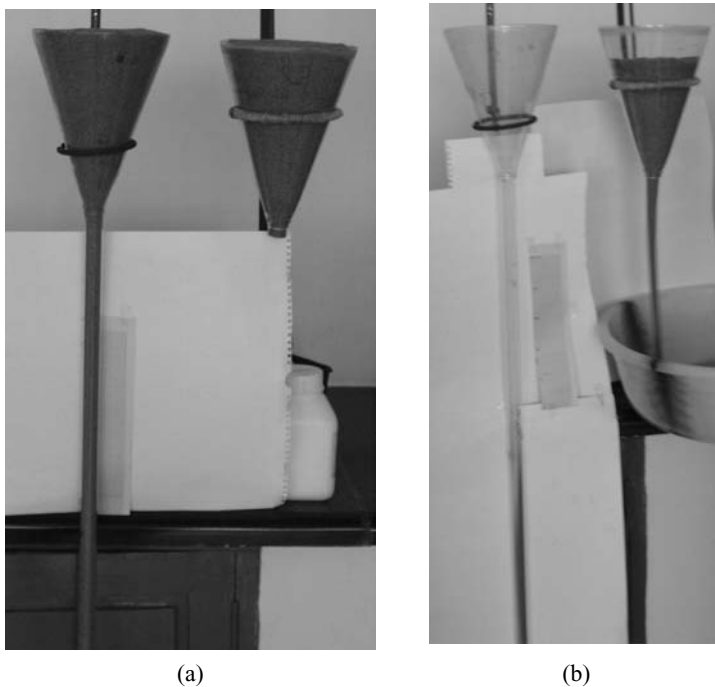


Figure 1.9. (a) A glass hopper–standpipe combination (HS) and a bare glass hopper (H) filled with sand. (b) Photograph taken during discharge of the granular material. Time required for complete discharge of the material = 9.7 s (HS), 14.4 s (H). Parameter values: particle diameter = 0.5–1.2 mm, inner diameter of the standpipe = 20.9 mm, length of the standpipe = 1.17 m, wall angle of the hopper section of the standpipe $\approx 18^\circ$, diameter of the exit orifice of the hopper = 21.1 mm, wall angle of the hopper $\approx 16^\circ$, initial mass of the granular material = 2.85 kg (HS), 2.55 kg (H). This experiment was set up by Mr. J. Ravi Prakash and Mr. P. T. Raghuram.

Introduction

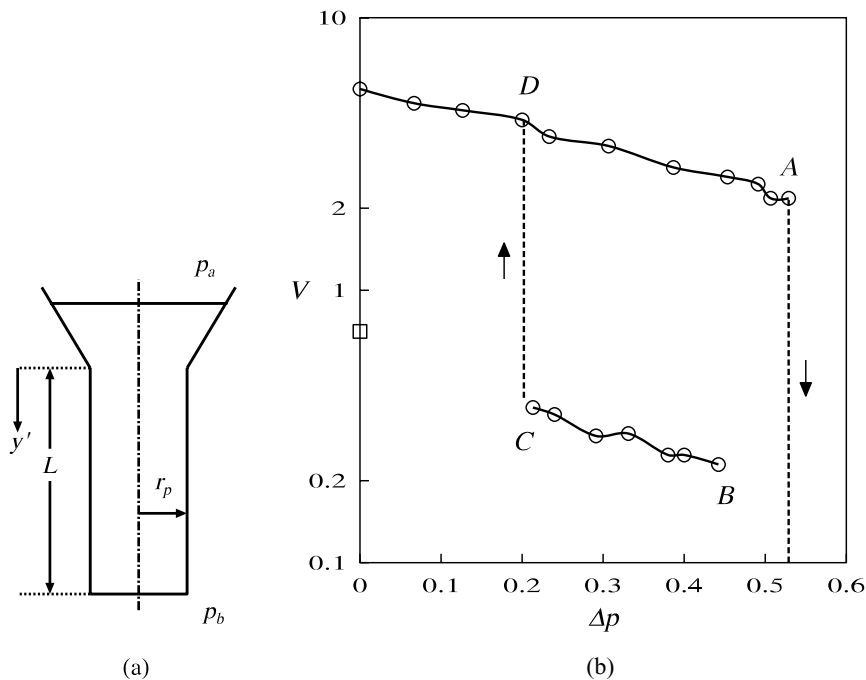


Figure 1.10. (a) A standpipe connected to a hopper. The pressure of the air is p'_a at the top of the hopper and p'_b at the bottom of the pipe. (b) Variation of the dimensionless mass flow rate V with the dimensionless pressure rise $\Delta p \equiv p_b - p_a$ for the flow of sand: \circ , data of Chen et al. (1984); —, curve drawn to guide the eye. Here p_a and p_b are the dimensionless air pressures. The mass flow rate is scaled by $\rho_p v_0 \pi r_p^2 \sqrt{g r_p}$ and the pressure by $\rho_p v_0 g L$, where ρ_p is the particle diameter, g is the acceleration due to gravity, r_p and L are the inner radius and length of the pipe, respectively, and v_0 is the solids fraction of a moving bed of particles. The square in (b) denotes the dimensionless mass flow rate for a bare hopper. Parameter values: $\rho_p = 2,620 \text{ kg m}^{-3}$, $r_p = 25.4 \text{ mm}$, $L = 3.27 \text{ m}$, $v_0 = 0.64$, mean diameter of sand = $154 \text{ }\mu\text{m}$.

from both the devices, shows that the hopper section of the hopper–standpipe combination was empty, whereas the bare hopper was nearly full (Fig. 1.9b). It is striking that the average mass flow rate from the former was about 70% larger than that from the latter. The use of a long pipe to increase the flow rate of granular material from a hopper was first reported by Bingham and Wikoff (1931).

Before discussing the reasons for this behavior, let us consider the experiments of Chen et al. (1984) on the flow of sand through a vertical standpipe connected to a hopper (Fig. 1.10a). The flow rate of the particles can be controlled by adjusting the pressure rise $\Delta p' \equiv p'_b - p'_a$, where p'_a and p'_b are the pressure of the air at the top of the hopper and the bottom of the pipe, respectively. Alternatively, the flow rate can be controlled by the orifice size of a slide valve located at the bottom of the pipe. Here we consider the case of a fully open valve, i.e., the orifice diameter is equal to the inner diameter of the pipe.

The circles in Fig. 1.10b show the variation of the dimensionless mass flow rate of particles $V = \dot{m}/(\rho_p \pi r_p^2 \sqrt{g r_p})$ with the dimensionless pressure rise ($\Delta p = (p'_b - p'_a)/(\rho_p v_0 g L)$), where \dot{m} is the mass flow rate, ρ_p is the particle density, r_p is the radius of the pipe, g is the acceleration due to gravity, and $v_0 = 0.64$ is the solids fraction corresponding to the random close packing of uniform spheres. Let us first discuss the case $\Delta p = 0$. The flow rate obtained using the bare hopper, shown by the square in Fig. 1.10b, is about seven times lower than the value obtained using the hopper–standpipe combination.

The reason for the enhanced flow rate in the latter case can be understood by examining the profiles of the pressure of the interstitial air. Fig. 1.11a shows the profile

Introduction

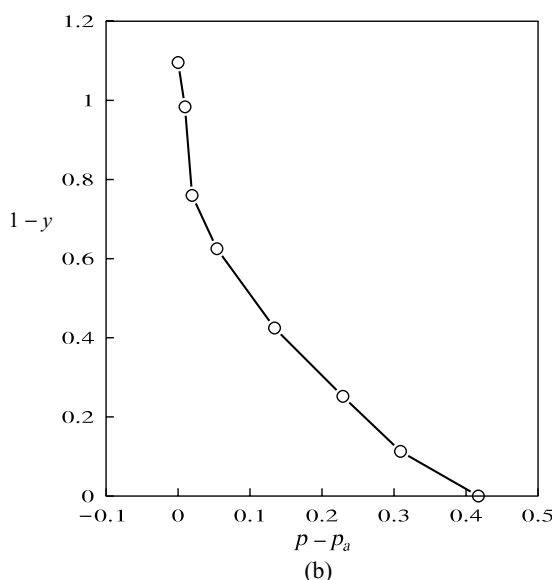
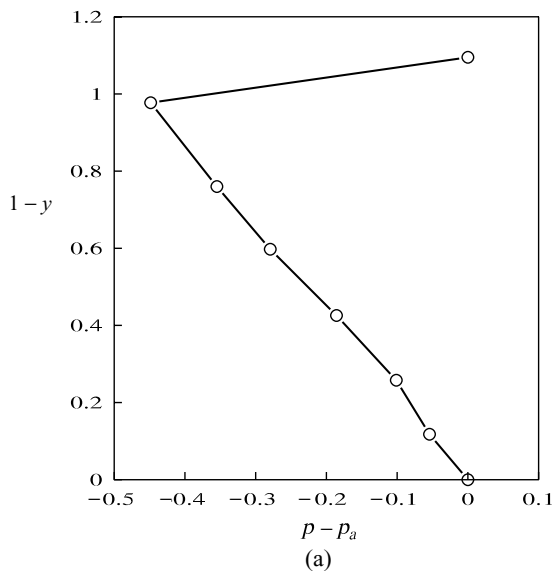


Figure 1.11. Profile of the dimensionless pressure p of the interstitial air for (a) the point on the upper branch of the curve shown in Fig. 1.10b, with $\Delta p \equiv p - p_a = 0$ and (b) the point on the lower branch of the curve with $\Delta p = 0.4$: \circ , data of Chen et al. (1984); —, curve drawn to guide the eye. Here p_a is the dimensionless air pressure at the top of the hopper, $y = y'/L$, y' is the vertical coordinate measured as shown in Fig. 1.10a, and L is the length of the standpipe.

obtained by measuring the pressure of the interstitial air at various points along the wall of the pipe during the discharge of sand. The dimensionless pressure at $y = 0$, the junction between the standpipe and the hopper, is less than the atmospheric pressure p_a , whereas it is equal to p_a at the top of the hopper. Hence the pressure gradient exerted by the air on the particles aids gravity within the hopper and opposes it within the standpipe. In contrast, just above the exit slot of a bare hopper, there is an adverse pressure gradient of the interstitial air (Spink and Nedderman, 1978). Hence the material discharges faster from the hopper section of the hopper–standpipe system than from a bare hopper. Now consider the pipe, which is equivalent to a hopper with vertical walls. As discussed in §3.3, the pipe is likely to discharge material at a higher rate than the hopper. If this enhancement is larger than the reduction caused by the adverse pressure gradient of the air in the pipe, the flow rate will be limited by the rate at which